



(51) International Patent Classification:

G01V 3/30 (2006.01) G01V 3/38 (2006.01)
E21B 47/00 (2012.01) G01V 3/18 (2006.01)

(21) International Application Number:

PCT/NO2020/050053

(22) International Filing Date:

28 February 2020 (28.02.2020)

(25) Filing Language:

English

(26) Publication Language:

English

(30) Priority Data:

1902794.5 01 March 2019 (01.03.2019) GB
1908345.0 11 June 2019 (11.06.2019) GB

(71) Applicant: EQUINOR ENERGY AS [NO/NO]; Forus-
been 50, 4035 Stavanger (NO).

(72) Inventor: STALHEIM, Stein Ottar; Skaretoppen 5, 5174
Mathopen (NO).

(74) Agent: LIND, Robert; Fletcher House, 2nd Floor, Heatley
Road, Oxford Science Park, Oxford Oxfordshire OX4 4GE
(GB).

(81) Designated States (unless otherwise indicated, for every
kind of national protection available): AE, AG, AL, AM,
AO, AT, AU, AZ, BA, BB, BG, BH, BN, BR, BW, BY, BZ,
CA, CH, CL, CN, CO, CR, CU, CZ, DE, DJ, DK, DM, DO,

DZ, EC, EE, EG, ES, FI, GB, GD, GE, GH, GM, GT, HN,
HR, HU, ID, IL, IN, IR, IS, JO, JP, KE, KG, KH, KN, KP,
KR, KW, KZ, LA, LC, LK, LR, LS, LU, LY, MA, MD, ME,
MG, MK, MN, MW, MX, MY, MZ, NA, NG, NI, NO, NZ,
OM, PA, PE, PG, PH, PL, PT, QA, RO, RS, RU, RW, SA,
SC, SD, SE, SG, SK, SL, ST, SV, SY, TH, TJ, TM, TN, TR,
TT, TZ, UA, UG, US, UZ, VC, VN, WS, ZA, ZM, ZW.

(84) Designated States (unless otherwise indicated, for every
kind of regional protection available): ARIPO (BW, GH,
GM, KE, LR, LS, MW, MZ, NA, RW, SD, SL, ST, SZ, TZ,
UG, ZM, ZW), Eurasian (AM, AZ, BY, KG, KZ, RU, TJ,
TM), European (AL, AT, BE, BG, CH, CY, CZ, DE, DK,
EE, ES, FI, FR, GB, GR, HR, HU, IE, IS, IT, LT, LU, LV,
MC, MK, MT, NL, NO, PL, PT, RO, RS, SE, SI, SK, SM,
TR), OAPI (BF, BJ, CF, CG, CI, CM, GA, GN, GQ, GW,
KM, ML, MR, NE, SN, TD, TG).

Published:

— with international search report (Art. 21(3))

(54) Title: ESTIMATING ELECTRICAL PERMITTIVITY

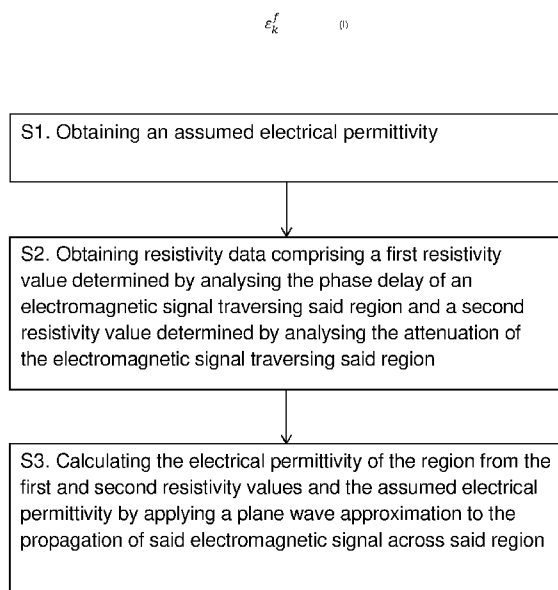


Figure 3

(57) Abstract: A method of determining the electrical permittivity (I) of a region of a subsurface formation surrounding a drilled borehole, the method comprises: obtaining an assumed electrical permittivity ϵ_{LWD} ; obtaining resistivity data comprising a first resistivity value R_p determined by analysing the phase delay δ of an electromagnetic signal traversing said region and a second resistivity value R_a determined by analysing the attenuation α of the electromagnetic signal traversing said region; and calculating the electrical permittivity of the region from the first and second resistivity values and the assumed electrical permittivity by applying a plane wave approximation to the propagation of said electromagnetic signal across said region.



ESTIMATING ELECTRICAL PERMITTIVITY

Technical Field

5 The present invention relates to a method of estimating the electrical permittivity in a subsurface formation and in particular to such a method that makes use of Logging While Drilling or Wireline obtained resistivity measurements.

Background

10

In analyzing and understanding geological formations in the context of hydrocarbon production, a key parameter that is considered by the petrophysicist is water saturation S_w . In a region that is under investigation (previously identified for example using a seismic survey), a high water saturation level will suggest that the level of recoverable hydrocarbons is low whilst a low water saturation level will suggest that the level of recoverable hydrocarbons is high. Put simply, hydrocarbon saturation is equal to $(1 - S_w)$. The estimation of water saturation influences major investment decisions including property acquisitions and divestment, infrastructure for extracting and transporting reserves, locating and planning new wells, defining data acquisition programs, completion decisions, reserves calculations, and stimulation programs. Estimating water saturation conventionally involves drilling into the region of interest while collecting data, a process known as Logging While Drilling (LWD), or collecting data using a wireline (WL) after drilling, and analyzing recovered (core) samples. One of the most commonly obtained data types using LWD and WL is electrical resistivity: in fact, resistivity is almost always obtained. Resistivity data typically comprises a phase (shift) resistivity R_p determined by analyzing the phase shift of an electromagnetic wave propagating through the formation, and an amplitude (attenuation) resistivity R_a determined by analyzing the attenuation of the electromagnetic wave. [In the case of an idealized, homogeneous formation the phase resistivity and the amplitude resistivity would be identical.] The term R_t is used below to refer to either phase resistivity or amplitude resistivity, and is referred to as the apparent bulk resistivity.

One method for estimating water saturation is described in Archie, G.E. 1942, "The Electrical Resistivity Log as an Aid in Determining Some Reservoir Characteristics", Trans. of AIME 146 (1): 54-62. This makes use of the following equation:

35

2

$$S_w = \left(\frac{R_w}{\phi^m \cdot R_t} \right)^{1/n}$$

where R_w is the water resistivity measured on water samples from the reservoir under investigation, R_t is the apparent bulk resistivity obtained by logging (LWD or WL), ϕ is the total porosity calculated by density log acquired by LWD or Wireline, m is the cementation exponent, and n is the saturation exponent (where m and n are empirically derived constants). The downside of Archie's approach is that it requires both water samples and core samples and is also subject to errors resulting from incorrect estimation of m and n .

Typically the raw LWD measurements are used as inputs to an inversion process which involves iteratively refining estimates of resistivity R_t to produce a resistivity model that corresponds to the raw measurement data and which can then be used to estimate water saturation (using for example Archie). The inversion process takes into account details of tool physics (e.g. geometry, antenna, tool calibration, environment correction, borehole correction, skin correction, correction for geometrical scattering) (Clark 1988, Clark 1990, ..). It is known to improve such inversion processes by incorporating electrical permittivity. This can be obtained using the conventional LWD or WL. [NB. LWD and WL operations are usually performed for a customer, e.g. the operator of an oil and gas field, by a service provider. In the absence of a detailed knowledge of tool physics it is difficult or impossible for such an operator to accurately apply an inversion process to the raw data.]

An alternative approach that relies on formation permittivity rather than resistivity is described in Complex Refraction Index Model, CRIM, (Hizem et al. 2008. "Dielectric Dispersion: A New Wireline Petrophysical Measurements". SPE 116130.). CRIM uses the weighted sum of the wavenumber to calculate the water saturation. For very high frequency, i.e. at GHz range, where there are minimum conductive losses and the polarization is small [the imaginary part in $\hat{k}^2 = \omega^2 \mu \epsilon \left[1 + i \frac{\sigma}{\omega \epsilon} \right]$ goes to 0], CRIM is reduced to the weighed sum of permittivity to the individual elements in the formation and the water saturation can be defined by.

$$S_w \cdot \phi \approx \frac{\sqrt{\epsilon_{formation}^*}}{\sqrt{\epsilon_{water}^*}}$$

where $\epsilon_{formation}^*$ is the apparent bulk permittivity measured on wireline, and ϵ_{water}^* is the permittivity to formation water measured from previously obtained samples or sometimes assumed to be a constant (between 50 and 80). CRIM makes use of

measurements obtained with a special dielectric wireline tool that measures the formation permittivity at a very high frequency, between 20 MHz and 1 GHz. Due to this high frequency, the water saturation is calculated only up to a very shallow in the formation, i.e. on a centimetre scale. The result is therefore not always representative for a non -
5 invaded formation (i.e. the formation that has not been invaded by drilling mud.

With a large amount of water this model can be quite inaccurate mainly due to uncertainties in ϵ_{water}^* . Whilst the CRIM approach does not require core or water samples (at least from the formation under investigation), it does require a complicated
10 water model for ϵ_{water} that depends on salinity, temperature and pressure and which is generally known only to the service provider and not the data customer, e.g. the field operator.

Summary

15

It is desirable to improve the accuracy with which water saturation for a region can be determined, and to perform such a determination using resistivity data that is conventionally provided by a service vendor to a data user such as an oil and gas field operator.

20

A method of estimating the water saturation level S_w of a region of a subsurface formation surrounding a drilled borehole. The method comprises obtaining resistivity data determined by analysing the attenuation α of an electromagnetic signal traversing said region and taking into account an assumed electrical permittivity value ϵ_{LWD} (normally
25 the assumption about electrical permittivity used by the service provider in data processing), and applying a plane wave approximation to the propagation of said electromagnetic signal across said region to extract an imaginary k_i part of a wave number k from the resistivity data and said assumed electrical permittivity value. The extracted imaginary part of the wave number is then used to calculate water saturation S_w .

30

It is noted that method may not require the evaluation of the extracted imaginary k_i part itself, but rather may incorporate the equations for deriving this component into an equation for calculating the water saturation S_w .

35

The resistivity data is data obtained by Logging While Drilling or by Wireline and using

one or more electromagnetic transmitter and receiver pairs, wherein the transmitter to receiver, TRS, spacing satisfies the condition:

$$\lambda/4\pi < TRS < \lambda,$$

where λ is the wavelength of the transmitted electromagnetic signal.

5

The resistivity data may comprise one or both of a phase resistivity R_p and an amplitude resistivity R_a .

10

The method may comprise performing a Logging While Drilling operation or a Wireline operation to obtain said resistivity data.

15

According to a second aspect of the present invention there is provided a method of drilling a borehole and comprising carrying out Logging While Drilling to obtain resistivity data using the method of the above first aspect to estimate the water saturation level S_w of a region being drilled, and geo-steering a drill bit using the estimated water saturation level to achieve optimal placement of the borehole.

20

According to a third aspect of the present invention there is provided a method of estimating the hydrocarbon saturation level S_{HC} of a region of a subsurface formation surrounding a drilled borehole, the method comprising estimating the water saturation level S_w of said region using the method of the above first aspect and using that estimate to estimate said hydrocarbon saturation level.

25

According to a fourth aspect of the present invention there is provided method of managing a hydrocarbon producing reservoir and comprising determining a water saturation level or determining a hydrocarbon saturation level according to one of the above aspects, and using the determined water or hydrocarbon saturation level to determine the location and /or orientation of wells into the reservoir, or to determine extraction or injection strategies for the reservoir.

30

According to a fifth aspect of the present invention there is provided a method of estimating the water saturation level S_w or hydrocarbon saturation level of a region of a subsurface formation surrounding a drilled borehole, the method comprising evaluating the following equation:

5

$$S_w = \frac{\omega \sqrt{\mu \varepsilon_{LWD}} \left[\frac{1}{2} \left(\sqrt{1 + \left(\frac{1}{\omega \cdot R_a \varepsilon_{LWD}} \right)^2} - 1 \right) \right]^{1/2}}{k_{wi} \cdot \phi}$$

, where S_w is the water saturation, k_{wi} is a constant, ϕ is porosity, ω is the angular frequency of a transmitted electromagnetic signal, μ is the electrical permeability, ε_{LWD} is the assumed permittivity value, R_a is a resistivity value of the resistivity data.

5

According to a sixth aspect of the present invention there is provided a method of determining the electrical permittivity ε_k^f of a region of a subsurface formation surrounding a drilled borehole, the method comprises:

obtaining an assumed electrical permittivity ε_{LWD} ;

10

obtaining resistivity data comprising a first resistivity value R_p determined by analysing the phase delay δ of an electromagnetic signal traversing said region and a second resistivity value R_a determined by analysing the attenuation α of the electromagnetic signal traversing said region; and

calculating the electrical permittivity of the region from the first and second resistivity values and the assumed electrical permittivity by applying a plane wave approximation to the propagation of said electromagnetic signal across said region.

15

The resistivity data can be obtained by Logging While Drilling (LWD) using one or more electromagnetic transmitter and receiver pairs, wherein the transmitter to receiver spacing (TRS) is within the radiative zone of the near field region of the or each transmitter.

20

The resistivity data can be obtained by Logging While Drilling (LWD) using one or more electromagnetic transmitter and receiver pairs, wherein the transmitter to receiver spacing (TRS) satisfies the condition:

25

$$\lambda/4\pi < TRS < \lambda,$$

where λ is the wavelength of the transmitted electromagnetic signal, and wherein an antenna of the or each transmitter is equal to or shorter than half the wavelength.

The step of calculating the electrical permittivity may comprise calculating the electrical permittivity according to the following equation:

30

$$\varepsilon = \frac{1}{2} \cdot \varepsilon_{LWD} \cdot [2 + A_p - A_a]$$

, where ε is the calculated electrical permittivity, ε_{LWD} is the assumed electrical permittivity, A_p is a term determined by the first resistivity value, and A_a is a term determined by the second resistivity value, wherein A_p and A_a may be given by

$$A_p = \sqrt{1 + \left(\frac{1}{\omega \cdot R_p \cdot \varepsilon_0 \cdot \varepsilon_{LWD}} \right)^2}$$

$$A_a = \sqrt{1 + \left(\frac{1}{\omega \cdot R_a \cdot \varepsilon_0 \cdot \varepsilon_{LWD}} \right)^2}$$

, where ω is the angular frequency of the electromagnetic signal, R_p is the first resistivity value, R_a is the second resistivity value, and ε_0 is the electrical permittivity of free space.

The step of calculating the electrical permittivity may comprise:

extracting a real part k_r and an imaginary part k_i of a wavenumber from the resistivity data;

10 using the real and imaginary parts to calculate the electrical permittivity.

The step of using the real and imaginary parts can comprise calculating the electrical permittivity according to the following equation:

$$\varepsilon = \left(\frac{c}{\omega} \right)^2 \cdot \frac{k_r^2 - k_i^2}{\mu}$$

, where ε is the calculated electrical permittivity, c is the speed of light in vacuum, ω is the angular frequency of the electromagnetic signal, k_r is the real part of the wavenumber, k_i is the imaginary part of the wavenumber, and μ is the relative permeability of the formation in said region.

The calculated electrical permittivity can be used to calculate new resistivity values from the phase delay and the attenuation of the electromagnetic signal.

The resistivity data may comprise further resistivity values determined from the phase delay and attenuation of another electromagnetic signal that traversed said region and having a different frequency, and wherein the method further comprises calculating another electrical permittivity of the region from the further resistivity values.

The calculated electrical permittivity can be used to determine a water saturation S_w of the region of the formation.

- 5 The method may further comprise drilling the borehole, wherein said step of calculating the electrical permittivity is performed while drilling.

The method may comprise geo-steering a drill bit using the determined electrical permittivity to achieve an optimal placement of the borehole.

10

According to a seventh aspect of the present invention there is provided a computer device comprising:

a receiver for receiving electromagnetic data; and

a processor arranged to carry out the method of any one of the preceding

15

claims.

According to an eighth aspect of the present invention there is provided a computer program comprising non-transitory computer readable code which, when run on a computer device, causes the computer device to behave as a computer device according to the seventh aspect.

20

According to a further aspect of the present invention there is provided a computer program product comprising a non-transitory computer readable medium and a computer program according to the eighth aspect, wherein the computer program is stored on the non-transitory computer readable medium.

25

Brief Description of the Drawings

Figure 1 illustrates zones of a region surrounding a borehole as a function of wavelength for an antenna that is equal to or shorter than half the wavelength transmitted by the antenna;

30

Figure 2 illustrates schematically LWD in a deviated well;

Figure 3 is a flow chart illustrating a method of determining the electrical permittivity from resistivity data;

Figure 4 illustrates schematically a known LWD tool and method for collecting data to determine resistivity;

35

Figure 5 shows an exemplary curve used to account for the impact of the electrical permittivity ϵ on the processed (inverted) resistivity;

Figure 6 illustrates zones of a region surrounding a borehole as a function of wavelength; and

5 Figure 7 is a flow chart illustrating a method of determining a water saturation level from LWD or WL obtained resistivity data.

Detailed Description

10 **Determination of electrical permittivity**

The electrical permittivity (ϵ) of rock can be measured and applied in petrophysical evaluation. With new-generation dielectric tools the popularity and application of ϵ has increased in the past years. One of the advances of the new-generation tools is the
15 measurement of ϵ at multiple frequencies (f), also known as the dispersive permittivity ($\epsilon(f)$). Applications of such data include pore-fluid analysis, water saturation calculation, matrix analysis like Archie's m , and shaly sand evaluation including clay volume calculations. Drawbacks with the dielectric tools are that they respond to the invaded zone (a few cm into the formation), and the data must be acquired on wire-line
20 and is therefore not always accessible.

Logging While Drilling (LWD) propagation resistivity records the phase shift and attenuation between two receivers and responds differently to the electrical rock properties (resistivity, permittivity and permeability). The characteristics of the
25 amplitude decay and the phase shift can therefore, under given conditions, be used to extract both the electrical permittivity and the resistivity from the measurements.

Information about ϵ and $\epsilon(f)$ is hidden in the LWD resistivities and can be extracted from the LWD resistivities. The (improved) permittivity determined in this way can be
30 acquired in real time and can be used to identify bypass zones, as geological marker and for geo-steering. The LWD resistivity accuracy can also be improved by replacing the empirical based assumption about ϵ (i.e. the initial estimate of $\epsilon = \epsilon_{LWD}$) with the more correct value of ϵ in the LWD processing. The improvement in accuracy of the LWD resistivity can be significant in rocks with large permittivity (e.g. organic-rich
35 source rock).

Electrical properties of a formation determine its response to an electromagnetic (EM) field. The electrical properties are the electrical conductivity (σ), the electrical permittivity ($\epsilon\epsilon_0$) and the electrical permeability ($\mu\mu_0$). μ is the relative electrical permeability and is the measure of the magnetization of the substance and μ_0 is the free space electrical permeability. Since magnetic materials are rarely found in oil and gas reservoirs, μ can usually be assumed to be unity and independent of the formation properties. σ is the conductivity (inverse of the resistivity (R_t)) and is the measure of the formations ability to conduct electric current. σ is heavily related to the amount of saline water (free charges) in formation and is a key input for calculation of formation water saturation (e.g. by use of Archie's equation). ϵ is the relative electrical permittivity and is the measure of the polarization of the formation and is the prominent characteristic of dielectric substances. ϵ_0 is the free space electrical permittivity. Due to strong polarization of water molecules compared with other substances in the formation, ϵ is strongly related to the amount of water in the formations and can be used to calculate formation water saturation (e.g. by use of a Complex Refraction Index Model, CRIM).

LWD operates at 2 or 3 frequencies and provide two independent, apparent resistivities. One from phase shift (R_p) and one from the amplitude decay (R_a) measurements. A set with R_p and R_a is processed for each f and for each Transmitter to Receiver Spacing (TRS). The characteristics of R_p and R_a depend on the electrical properties, which in practice are the resistivity and the permittivity when the relative permeability (μ) is unity. The resistivity and permittivity can therefore in principle be simultaneously inverted out from the phase and amplitude measurements.

When determining LWD resistivity an empirically derived resistivity dependent (initial) permittivity ϵ_{LWD} is used. If the estimated/assumed permittivity ϵ_{LWD} (normally the assumption about electrical permittivity used by the service provider in data processing) does not accurately represent the permittivity of rock being measured, it introduces systematic error in the generated R_p and R_a . This is known as the dielectric effect. The error is most pronounced in high resistivity zones, and R_a is more sensitive to ϵ compared with R_p . The error can be significant with R_a above 10 Ohm-m and with R_p above 100 Ohm-m. Aiming to reduce the dielectric effects on R_p and R_a , a couple of algorithms that simultaneously inverts out both resistivity and permittivity have been developed. These algorithms use raw measurements of the phase shift and attenuation

as inputs to an inversion process together with detailed knowledge of the complexity of tool physics (tool and antenna geometry, tool calibration, environment correction, borehole correction, skin correction, correction for geometrical scattering etc.). The LWD amplitude and phase measurements are assumed to have a high accuracy and the processed LWD resistivities, R_p and R_a , can therefore also be assumed to be accurate.

The relation between R_p , R_a and the LWD amplitude and phase measurements is described by the electromagnetic wave properties. In embodiments described herein, a plane wave approximation is used to determine the relative electrical permittivity from R_p , R_a and ε_{LWD} . For electromagnetic plane waves all corresponding wave properties can be derived from the wavenumber. For an isotropic formation (where electrical properties are scalar) the wavenumber is

$$\hat{k}^2 = \omega^2 \mu \mu_0 \varepsilon \varepsilon_0 \left[1 + i \frac{\sigma}{\omega \varepsilon \varepsilon_0} \right] = (k_r + ik_i)^2 \quad (1)$$

, where the hat, $\hat{}$, stands for complex number, ω is the angular frequency, i is the pure imaginary number $\sqrt{-1}$, and k_r and k_i are the real and imaginary part of \hat{k} respectively. An expression for σ and ε is found by decomposing \hat{k} (equation 1) into the real and imaginary parts

$$k_r^2 - k_i^2 = \omega^2 \mu \mu_0 \varepsilon \varepsilon_0 \quad (2)$$

$$2 \cdot k_r \cdot k_i = \omega \cdot \mu \mu_0 \cdot \sigma \quad (3)$$

, and solve with respect to σ and ε

$$\sigma = \frac{2k_i k_r}{\omega \mu \mu_0} \quad (4)$$

$$\varepsilon = \left(\frac{c}{\omega i} \right)^2 \cdot \frac{k_r^2 - k_i^2}{\mu} \quad (5)$$

, where c is the speed of light in vacuum, $c = \frac{1}{\sqrt{\varepsilon_0 \mu_0}}$. For a non-magnetic formation μ is equal to 1, and σ (equation 4) and ε (equation 5) can be calculated if k_r and k_i are known. Equation 4 and 5 are known as such, but how to obtain k_r and k_i from LWD resistivity, as is described herein, is not. Embodiments described herein allow for the deduction of k_r and k_i from LWD resistivity measurements and application of equation 5 to determine the permittivity from k_r and k_i .

The present method to calculate k_r and k_i is based on a plane wave model of the electrical field (E) given by

$$\begin{aligned}\bar{E}(z, t) &= \hat{x}\bar{E}_x(z, t) = \text{Re}\{\hat{x}E_0 e^{-k_i z + i k_r z} e^{-i\omega t}\} \\ &= \hat{x}E_0 e^{-k_i z} \cos(k_r z - \omega t)\end{aligned}\quad (6)$$

, where z is the position, t is time and E_0 is the electrical field strength at $z = t = 0$. \hat{x} is the direction of the E-field and is perpendicular to the direction of propagation. Equation 6 describes a wave that propagates in the direction of k_r and with amplitude decrease most rapidly in the direction of k_i . k_i represents the energy loss. Equation 6 shows that k_r describes the phase behaviour and k_i describes the amplitude behaviour of the E-field. Since R_p is processed from the phase shift it is linked to k_r , while R_a is processed from the amplitude decay and is linked to k_i . The relations between k_r and R_p , and between k_i and R_a , is found by the general solutions for k_r and k_i by solving equation 2 and 3 with respect to k_r and k_i

$$k_r = \frac{\omega}{c} \sqrt{\mu\epsilon} \left[\frac{1}{2} \left(\sqrt{1 + \left(\frac{\sigma}{\omega\epsilon\epsilon_0} \right)^2} + 1 \right) \right]^{1/2} \quad (7)$$

$$k_i = \frac{\omega}{c} \sqrt{\mu\epsilon} \left[\frac{1}{2} \left(\sqrt{1 + \left(\frac{\sigma}{\omega\epsilon\epsilon_0} \right)^2} - 1 \right) \right]^{1/2} \quad (8)$$

In order to determine k_r and k_i from LWD measurements, they can be calculated using equation 7 and 8 and with $\sigma = 1/R_p$ for k_r (equation 7) and with $\sigma = 1/R_a$, for k_i (equation 8). For ϵ , the initial estimate of permittivity normally provided by the vendor ($\epsilon = \epsilon_{LWD}$) is used. Putting $k_r(R_p, \epsilon_{LWD})$ (equation 7) and $k_i(R_a, \epsilon_{LWD})$ (equation 8) into equation 4 and 5 gives

$$\sigma = \omega \cdot \epsilon_0 \cdot \epsilon_{LWD} \cdot \left[(A_p + 1)^{1/2} \cdot (A_a - 1)^{1/2} \right] \quad (9)$$

$$\epsilon = \frac{1}{2} \cdot \epsilon_{LWD} \cdot [2 + A_p - A_a] \quad (10)$$

, where

$$A_p = \sqrt{1 + \left(\frac{1}{\omega \cdot R_p \cdot \epsilon_0 \cdot \epsilon_{LWD}} \right)^2} \quad (11)$$

$$A_a = \sqrt{1 + \left(\frac{1}{\omega \cdot R_a \cdot \epsilon_0 \cdot \epsilon_{LWD}} \right)^2} \quad (12)$$

, where Equation 9 and 10 are analytic equations for determining the conductivity and relative permittivity of a formation using LWD R_p and R_a , and ϵ_{LWD} as input. The conductivity σ and relative permittivity ϵ determined by equation 9 and 10 can be referred to as σ_k^f and ϵ_k^f respectively, where index k indicates that σ and ϵ are calculated with the wavenumber (using the plane wave approximation). Index f indicates the frequency at which σ and ϵ are calculated. For example, ϵ_k^{2MHz} is the permittivity calculated by use of equation 10 at a frequency of 2 MHz.

Equation 9 and 10 is based on a plane wave model (equation 6) in an isotropic medium (equation 1), and physical zones for where these conditions are sufficiently fulfilled should be considered when applying the method to a formation. Equation 6 is an example of a plane wave and will in practice be valid when the receiver is located at a sufficiently great distance away from the transmitter and a sufficiently great distance from free charges. An isotropic medium is where the electrical properties can be treated as scalar (ϵ , σ , μ). Since equation 1 and following equations are scalar, the present results are valid for isotropic media. Since the E -field behaves differently depending on the distance from the source, the E -field is classified into regions as a fraction of the wavelength, λ . Equation 6 show that λ is

$$\lambda = \frac{2 \cdot \pi}{k_r} \quad (13)$$

k_r is given by equation 7. Elementary considerations such as by examination of the E field of a dipole radiator show that there are three zones that may be considered. The near-field, or static, zone, where the Transmitter to Receiver Spacing (TRS) is small compared with λ , the transition zone where $TRS \sim \lambda$, and the radiation zone where $TRS \gg \lambda$. There is no clear cut-off between these regions and they will in practice depend on the physical size of the antenna. For antennas equal to or shorter than one-half wavelength of the radiation they emit, it is common to classify the physical zone as

illustrated by Figure 1. This classification is assumed to be a good approximation for LWD frequencies.

5 In the reactive part of the near field zone, close to the transmitter, the EM-field is heavily influenced by the transmitter, and the plane wave model shown is not valid. It will therefore be a minimum TRS for where a plane wave approximation can be expected and embodiments of the described method can be used to accurately determine the permittivity ϵ_k^f . For example, the described method should not be used with LWD measurements within the reactive part of the near field where $TRS < \lambda/4\pi$.
10 The reactive part of near-field is illustrated by red colour in Figure 1.

The radiative part of the near field can be approximated as quasi-static and pertains to low frequency situations in which the applied EM field varies slowly with time. The characteristic feature here is that the wavelength, λ , is large compared with the dimensions/volume (TRS) of the rock that is being measured. Equation 9 and 10 can be used with LWD measurements in the radiative part of the near field where $\lambda/4\pi < TRS < \lambda$. That is, embodiments of the described method can be used to accurately determine the conductivity σ_k^f and permittivity ϵ_k^f for at least $\lambda/4\pi < TRS < \lambda$. The radiative part of the near field is illustrated by orange colour in Figure 1.
20

The validity of the described method can be difficult to assess in the transition zone, since there is no clear cut-off between the near field and the far field zones. In the transition zone the EM field can behave like the radiative part of the near field, or like the far field or something in between. The transition zone is illustrated by light green colour in Figure 1.
25

In the far field zone, where $\lambda \ll TRS$, the EM radiation will dominate, and the E-field will be more sensitive to absorption and scattering. The far field is illustrated by green colour in Figure 1.

30 If the formation is anisotropic, reflection and refraction is expected if the angle of incident (θ_1) does not exceed the critical angle of total reflection (θ_c). The principle is illustrated by Figure 2. In such situations the refracted k_r and k_i will have different direction. This is explained by the phase match principle and Snell's law. From the

phase match principle, k_i will always be perpendicular to the conducting surface, while related to Snell's law k_r is refracted by a real refraction angle Θ_2 .

5 For LWD measurements in the radiative zones where $\lambda/4\pi < TRS$, equation 9 and 10 is expected to:

- Fail in anisotropic formation where the angle of incidence θ_1 is less than critical angel for total reflection, θ_c .
- Fail when the E -field crosses into a new formation with electrical contrasts/discontinuity and $\theta_1 < \theta_c$.
- 10 • Be valid in isotropic medium where there is no electrical contrast, or where the angle of incidence is larger than the critical angle θ_c .

Note that θ_c is a function of the electrical contrasts and can be quite large.

15 Figure 3 illustrates the steps of a method of determining the electrical permittivity ϵ_k^f of a region of a subsurface formation surrounding a drilled borehole according to an embodiment. The method comprises obtaining an assumed electrical permittivity ϵ_{LWD} (step S1) and obtaining resistivity data comprising a first resistivity value R_p determined by analysing the phase delay δ of an electromagnetic signal traversing said region and a
 20 second resistivity value R_a determined by analysing the attenuation α of the electromagnetic signal traversing said region (step S2). The method further comprises calculating the electrical permittivity of the region from the first and second resistivity values and the assumed electrical permittivity by applying a plane wave approximation to the propagation of said electromagnetic signal across said region (step S3). The method
 25 is a computer implemented method, wherein the computer comprises a processor for processing input data (R_p , R_a , ϵ_{LWD}) and generating output data (ϵ_k^f). In particular for geo-steering applications, sufficient computational capacity is required to process the data in real time. The input data can be stored in memory on the computer where it can be accessed by a processor, which applies equations 10, 11 and 12 to the input data to
 30 generate the output data.

Determination of water saturation

The Complex Refraction Index Model (CRIM) is the weighted sum of the wavenumber
 35 to the elements in the formation

$$\hat{k} = \hat{k}_w \cdot \phi \cdot S_w + \hat{k}_m \cdot (1 - \phi) + \hat{k}_{hc} \cdot \phi \cdot (1 - S_w) \quad (14)$$

, and is used to calculate the amount of water (S_w). Index w is water, m is matrix and hc is hydrocarbon. ϕ is the porosity. A high frequency approximation of CRIM can be used when calculating S_w . Using the high frequency approximation, the wavenumbers in equation 14 are replaced by the permittivity's only (i.e. at very high frequency, in equations 7 and 8, $\frac{\sigma}{\omega \epsilon \epsilon_0} \approx 0$ and therefore $k_i \approx 0$ and $k_r \approx \frac{\omega}{c} \sqrt{\mu \epsilon} = \text{constant} \cdot \sqrt{\epsilon}$).

CRIM does not account for the interfacial polarization and is therefore in principle not valid at LWD frequencies. The interfacial polarization is also known as the Maxwell-Wagner polarization and is related to the presence of charges that is concentrated at the surface of the rock when electrical field is applied. The interfacial polarization is one of three main physical phenomena contributing to the permittivity. The interfacial polarization vanishes past a certain frequency which may be around 108 Hz. Since the LWD frequency is far below 108 Hz, the interfacial polarization will contribute to the electrical permittivity, and the wavenumber (equation 1).

15

Embodiments described herein provide a modified version of CRIM, which can be used at LWD frequencies by applying the imaginary part of the wavenumber. It is assumed that the impact of the interfacial polarization can be added to equation 14 as a new element. The new element is the wavenumber associated with the interfacial polarization, k_p , weighted by M_s . M_s is the volume water associated with the interfacial polarization at the surface of the matrix. The proposed modified CRIM is

20

$$\hat{k} = \hat{k}_w \cdot \phi \cdot S_w + \hat{k}_m \cdot (1 - \phi) + \hat{k}_{hc} \cdot \phi \cdot (1 - S_w) + \hat{k}_p \cdot M_s \quad (15)$$

Index p is interfacial polarization. Equation 15 can then be split into its real part and its imaginary part

$$k_r = k_{wr} \cdot \phi \cdot S_w + k_{mr} \cdot (1 - \phi) + \quad (16)$$

$$k_{hcr} \cdot \phi \cdot (1 - S_w) + k_{pr} \cdot M_s \quad (17)$$

$$k_i = k_{wi} \cdot \phi \cdot S_w + k_{mi} \cdot (1 - \phi) +$$

$$k_{hci} \cdot \phi \cdot (1 - S_w) + k_{pi} \cdot M_s$$

Since the conductivity of the matrix and of the hydrocarbon is zero, the value on k_{mi} and k_{hci} is zero (see equation 8). k_{pr} and k_{pi} can be calculated with equation 7 and 8 if the electrical properties associated with the interfacial polarization (σ_p , ε_p) is known. It can be assumed that that ε_p is large and that σ_p is small. σ_p is assumed to be small since the presence of charges that is concentrated at the surface of the rock is not free to move. With a large value for ε_p and small value for σ_p , the part $\sigma_p/(\omega\varepsilon_p\varepsilon_0)$ in equation 7 and 8 is expected to be very small and k_{pr} and k_i can be approximated by:

$$k_{pr} \approx \omega \cdot \sqrt{\mu_p \cdot \varepsilon_p} \quad (18)$$

$$k_{pi} \approx 0 \quad (19)$$

Use equation 19, $k_{mi} = k_{hci} = 0$ into equation 17, and solve with respect to S_w to give

$$S_w = \frac{k_i}{k_{wi} \phi} \quad (20)$$

k_i is calculated by use of equation 8 with LWD R_a and ε_{LWD} , and ϕ can be calculated by use of e.g. the density log. The value on k_{wi} can be calculated with equation 8 if the electrical properties to the formation water (σ_w , ε_w) is known, by in-situ calibration in a zone where the pore space is 100% filled with water, ($k_{wi} = k_i / \phi$), or extract it from the dispersion $k_r(f)$ and $k_i(f)$.

Embodiments of the method were applied to LWD resistivity data and compared with results from commercial wireline tools. Data from three different wells was used.

- Example 1: ε_k^f fit well with ε_{ADT}^f in vertical wells on data from different LWD vendors.
- Example 2: The value of k_r , and then the calculated ε_k^f , have a too low value in deviated wells, and need to be corrected.
- Example 3: The water saturation calculated by use of equation 20 fits well with water saturation calculated by use of conventional methods.

In all examples Schlumberger ADT tool is used to acquire wire-line permittivity data. ADT acquired permittivity at four different frequencies ϵ_{ADT}^{20MHZ} , ϵ_{ADT}^{80MHZ} , ϵ_{ADT}^{400MHZ} and ϵ_{ADT}^{1GHZ} .

5 Example 1:

10 It was shown that LWD permittivity and its dispersion fit well with permittivity data from commercial wire-line tools. To minimize the impact of anisotropy and refraction the examples are taken from two vertical wells. Both wells are drilled with oil-based mud. The first well comprises shale above a heterolithic hydrocarbon filled reservoir. The shale resistivity is approximately 2 Ohm-m and the reservoir resistivity is in the range from 2 - 10 Ohm-m. The LWD data was acquired by Halliburton which operates at frequencies, 125 kHz, 500 kHz and 2 MHz. ϵ_{LWD} was equal 10 for all frequencies. σ_k^f was calculate by equation 9 and ϵ_k^f was calculated by equation 10.

15 The LWD measurements were mainly acquired at the border in between the reactive and radiative part of the near field zone. ϵ_k^f had a continuous curve for all three frequencies, except for a few small intervals where ϵ_k^f was negative. The intervals where ϵ_k^f was negative occurred where the resistivity and ADT permittivity showed electrical contrasts. The measurements at the lowest frequencies, ϵ_k^{125kHz} was less influenced by electrical contrasts when compared to ϵ_k^{400kHz} and ϵ_k^{2MHz} . The broad-banded dispersion plot showed that the level of ϵ_k^f fit well in with the ϵ_{ADT}^f dispersion for measurements in the radiative part of the near field. The permittivity values that were obtained from measurements in the reactive part of the nearfield were slightly too high when compared to the dispersion trend given by the other measurements.

25

The other well comprised shale above a homogeneous hydrocarbon filled reservoir, with a water zone at the bottom. The shale resistivity was approximately 2 Ohm-m, the hydrocarbon filled reservoir resistivity was in the range from 100 to 200 Ohm-m, and the water filled formation resistivity was approximately 1 Ohm-m. The LWD data was acquired 30 by Schlumberger, at the frequencies 400 kHz and 2 MHz. ϵ_{LWD} was obtained as set out in the research article: Anderson B. I. et al. 2007. "Observations of large dielectric effects on LWD propagation-resistivity logs", SPWLA 48th Annual Logging Symposium:

$$\varepsilon_{LWD}^{2MHz} = 5 + 88.5 \cdot \left(\frac{\sigma}{\sigma_0}\right)^{0.35} \quad (21)$$

$$\varepsilon_{LWD}^{400kHz} = 5 + 280 \cdot \left(\frac{\sigma}{\sigma_0}\right)^{0.46} \quad (22)$$

The conductivity scale σ_0 is equal to 1. σ_k^f was calculated with equation 9 and ε_k^f was calculated with equation 10. The LWD measurements were acquired in the reactive near field and in the radiative part of the near field zone. $R_a^{f400kHz}$ was not accurate in the reactive part of the near field and the calculated value ε_k^f was not representative in this zone. For LWD measurements in the reactive part of the near field, ε_k^f showed a continuous curve but with too high values compared to the dispersion trend from the ADT measurements of permittivity. For LWD measurements in the radiative field zone, ε_k^f fluctuated. Where ε_k^f was positive it showed reasonable values. The negative values occurred where the LWD resistivity and ADT permittivity showed electrical contrast. The broad-banded dispersion plot showed that the level of ε_k^f dispersion fit in with the ε_{ADT}^f dispersion in the radiative zone.

Example 2:

It was shown that the value of k_r , and then the calculated ε_k^f (equation 5), had a too low value in deviated wells, which could, however, be corrected by the use of Snell's law. The tested well was a hetero-lithic hydrocarbon filled reservoir with shale above and below. The shale resistivity was approximately 1 Ohm-m and the reservoir resistivity was in the range of 5 to 10 Ohm-m. The well was drilled with oil-based mud and at an inclination of 30°. The LWD resistivities was acquired by Schlumberger and ε_{LWD} was given by equation 21 and 22. Only k_r was corrected for refraction by use of Snell's law. ε_k^f that was not corrected for refraction showed large intervals with negative values. In the intervals where it was positive, the permittivity values were too low compared to ε_{ADT}^f . ε_k^f that was corrected for refraction showed more continuous curves, and the permittivity values fit well with ε_{ADT}^f .

Example 3:

It was shown that the water saturation $S_w(k_i)$ calculated by the use of equation 20 agreed well with water saturation calculated by use of conventional methods. The conventional

methods used were Archie's equation to calculate the water saturation $S_w(Archie)$, water saturation delivered by Schlumberger ADT services $S_w(ADT)$, and water saturation calculated by use of nuclear magnetic resonance (NMR) $S_w(NMR)$. k_{wi} in equation 20 was 12.5 and found by calibration. The water saturation was determined in two wells using
 5
 10
 15
 20
 25
 30
 embodiments of the method described herein, and there was good agreement between $S_w(k_i)$, $S_w(Archie)$, $S_w(ADT)$ and $S_w(NMR)$ in both wells.

Embodiments herein provide new methods of determining the permittivity and water saturation in a formation. ε_k^f has several benefits compared to ε_{ADT}^f and many potential applications. An important benefit is that the LWD resistivity is acquired in nearly all drilled wells and that ε_k^f can be extracted from the LWD measurements without significant extra cost. ε_{ADT}^f is acquired on wire-line and can therefore often by technical and/or economical reason, not be accessible. Due the lower frequency, large TRS and shorter time between formation drilling and measurements, the LWD is far less affected by invasion of drilling mud when compare with the high frequency, short TRS dielectric wireline measurements. The values of ε_k^f can therefore be more representative of non-invaded formation, which is generally the target for petrophysical evaluation. Since ε_k^f and the wavenumber can be acquired in real time during drilling, it can be used proactively to identify bypass zone (equation 20) and it can be used as a geological marker (e.g. organic-rich source rock). This information can be useful for geo-steering purposes. In an embodiment, the determined permittivity is used to change a drilling operation. For organic-rich source rock or formation where the electrical permittivity is extremely high, 10 to 50 000 the error on the processed LWD R_a and R_p can be large due to dielectric effects. In such a case the formation resistivity can be calculated by use of k_r and k_i with equation 9. Equation 9 give the resistivity that is not influenced by the dielectric effect and will be more accurate compared with LWD R_a and R_p . Since the LWD resistivity and dielectric wireline measurements operate at different frequencies, they have different sensitivity to the different polarization mechanisms. Different polarization mechanisms include electronic polarization, molecular orientation and the interfacial polarization. The LWD dispersion permittivity ε_k^f is more sensitive for interfacial polarization and salinity to the formation water comparing with ε_{ADT}^f . This can allow information about the electrical properties of the formation water to be extracted, which is a key parameter in water saturation calculation from electrical logs. Use of $\varepsilon_k^f(f)$ may be used to extract information about

VSH, CEC, and Archie's m . $\varepsilon_k^f(f)$ can also be used together with $\varepsilon_{ADT}^f(f)$ to increase the bandwidth of dielectric dispersion.

5 The classification of physical zones can be used to optimize the electromagnetic tool configuration. The optimal zone for measurements is in the radiative part of the near field where $\lambda/4\pi < TRS < \lambda$. Since the value on λ (equation 7 and 13) is dynamic and is a function of the frequency and the electrical properties to the formation, an optimal electromagnetic tool should had the possibility to tune the frequency and/or TRS to be in the radiative near field zone, $\lambda/4\pi < TRS < \lambda$.

10

As has already been noted, electrical resistivity in terms of a phase and an amplitude resistivity is almost always obtained in Logging While Drilling (LWD) operations. Moreover, such data is typically provided by the service vendor (performing the drilling) to the data customer (together with an assumed permittivity ε_{LWD} used by the vendor to obtain the resistivities), e.g. the operator (license holder) of an oil and gas field. An approach to determining electrical permittivity ε and its dispersion $\varepsilon(f)$ from LWD resistivity measurements, and their use to calculate water saturation, will now be described. This approach relies upon the principle that information about the electrical permittivity and dispersive permittivity [where dispersive permittivity is the measurement of ε at multiple frequencies (f)] can be extracted from multi-frequency (amplitude and phase) resistivity measurements obtained by, for example, LWD (or WL). In one sense, ε and $\varepsilon(f)$ can be considered as being hidden in the already obtained resistivities, and as such there is little extra effort required to obtain the permittivity data. Moreover, the permittivity data can be acquired in real-time and can be used to identify bypass zones, as a geological marker, and for geo-steering while drilling. The approach differs from CRIM which requires the use of a special and costly dielectric wireline tool to measure permittivity and which can only look at a very shallow depth into the formation.

15

20

25

30

The LWD resistivity accuracy can also be improved by replacing the empirically-based assumption about ε with a more correct value in the LWD resistivity processing. This improvement in accuracy of the LWD (or WL) resistivity will be significant in rocks with large permittivity (e.g. organic-rich source rock). Results have been demonstrated to fit

extremely well with data obtained from commercial wireline tools (deployed after drilling).

LWD tools are well known and described, for example, in Clark. B. et al. 1990. “Electromagnetic Propagation Logging While Drilling: Theory and Experiment. “ SPE. Sept. 1990. Figure 4 illustrates schematically a tool and method for collecting LWD data. A borehole 1 has been drilled by a drill bit (not shown) attached to the bottom of a drill string 2. A tool is incorporated into the drill string and comprises a pair of radio frequency transmitters T1,T2 and a pair of radio frequency receivers R1,R2. The receivers are spaced apart from one another whilst being centrally located between the two transmitters. Although not shown, the tool comprises a transmitter capable of transmitting digital data to the surface using a mud-pulsing technique, as well as electronic components for logging collected data (whereby the data can be recovered from these components after the tool has been recovered to the surface). The tool further comprises components for determining the precise location, both in terms of depth and angle, of the tool and therefore of the transmitters and receivers.

The transmitters and receivers are configured to be in relatively close proximity to the formation but without making electrical contact therewith. The transmitters each generate RF electrical voltages V_0 that are inductively coupled to the formation. The receivers then detect these signals transmitted through the formation. Transmitters may be operated one at a time or in parallel. The graph on the right hand side of Figure 4 illustrates by way of example the RF signals that are detected by the receivers R1,R2 when the transmitter T1 is operated. As receiver R2 is further from the transmitter T1 than the receiver R1, the amplitude of the signal received by the receiver R2 is reduced by an amount $\alpha = \sigma_0 - \gamma_0$. The phase of the signal received by the receiver R2 is shifted by an angle δ compared to the phase of the signal received by the receiver R1. The voltage detected by a receiver can be expressed as:

$$V(z, t) = V_0 e^{-\alpha z + \delta z} e^{-i\omega t} \quad (23)$$

where z is the coordinate in space, t is time, ω is the angular frequency ($2\pi f$), i.e. the signal frequency used by the LWD tool (e.g. $f = 125\text{kHz}$, 400kHz , 500 kHz , 2MHz or frequencies in or around this range), and e is Euler’s number (2.72).

The conventional tool of Figure 4 therefore allows the amplitude decay and the phase shift of the transmitted signals (i.e. the “raw” measurements”) to be obtained for a

region of the formation surrounding the hole (extending perhaps one meter into the formation). Different sets of data can be obtained from the different transmitters, and the data combined to improve the quality of the results. The amplitude decay α and the phase shift δ are functions of the electrical properties of the formation (resistivity R_t ,
 5 permittivity ε , and permeability μ), i.e.

$$\alpha = f(R_t, \varepsilon, \mu) \quad (24)$$

$$\delta = f(R_t, \varepsilon, \mu)$$

As already discussed above, conventional approaches to determining water saturation
 10 use the raw measurements, α and δ , as inputs to an inversion process which involves iteratively refining estimates of (apparent) resistivity R_t to produce a resistivity model that corresponds to the raw measurement data. It is common practice to assume only a relatively small impact of the electrical permittivity ε on the processed (inverted) resistivity. Figure 5 shows an example model that may be applied (in effect, the curves
 15 of Figure 5 provide a scaling factor for resistivity using some determined permittivity/dielectric constant).

The approach presented here starts from the application of a simple plane wave approximation to the induced EM waves travelling through the formation (i.e. assuming
 20 that the waves have wavefronts (surface of constant phase) that are infinite parallel planes). This makes it possible to extract the permittivity ε directly from the LWD phase and amplitude resistivity (R_p and R_a) as supplied by the service vendor (and derived by the service vendor using an inversion process applied to α and δ and using an assumed permittivity ε_{LWD}).

25

For a simple plane wave, as set out in Ellis D. V, Singer J. M. 2008, "Well Logging for Earth Scientists". Springer; 2 edition, ISBN-10: 1402037384, the wavenumber k is given by:

$$\hat{k}^2 = \omega^2 \mu \varepsilon \left[1 + i \frac{\sigma}{\omega \varepsilon} \right] \quad (25)$$

30

Note that equation 25 uses μ and ε to denote the absolute permeability and permittivity and not the relative permittivity and permeability as in equation 1. Equation 25 can be reformulated to provide real and imaginary parts k_i and k_r and solved with respect to permittivity ε and conductivity σ (inverse of resistivity, R_t) as follows:

$$\varepsilon = \left(\frac{c}{\omega}\right)^2 \cdot \frac{k_r^2 - k_i^2}{\mu} \quad \text{and} \quad \sigma = \frac{2k_i k_r}{\omega \mu \cdot \mu_0} \quad (26)$$

where μ is the relative electrical permeability, c is the speed of light, i is the imaginary number ($\sqrt{-1}$), and μ_0 is the free space electrical permeability (a universal constant).

5 A plane wave approximation for the electrical field E travelling in a direction z and at time t at a receiver is given by:

$$\bar{E}(z, t) = \text{Re}\{\hat{x} \bar{E}_0 e^{-k_i z + k_r z} e^{-i\omega t}\} \quad (27)$$

where E_0 is the field at start time zero, z is the position in space, t is time, and x is the direction perpendicular to z . Here, k_i describes the damping/decay of the wave and k_r describes the phase shift of the wave. Equation (27) shows us that k_i is the amplitude and can be estimated using R_a , while k_r is the phase and can be estimated using R_p .

The real and imaginary parts of the wavenumber - see Equation (25) can be defined as follows:

$$15 \quad k_r = \omega \sqrt{\mu \varepsilon} \left[\frac{1}{2} \left(\sqrt{1 + \left(\frac{\sigma_p}{\omega \varepsilon}\right)^2} + 1 \right) \right]^{1/2}, \quad k_i = \omega \sqrt{\mu \varepsilon} \left[\frac{1}{2} \left(\sqrt{1 + \left(\frac{\sigma_a}{\omega \varepsilon}\right)^2} - 1 \right) \right]^{1/2} \quad (28)$$

Equation (28) shows the mathematical relation between k_r and R_p ($=1/\sigma_p$) and between k_i and R_a ($=1/\sigma_a$). ε is known and equal ε_{LWD} . Equation 28 is similar to equation 7 and 8 but using μ and ε to denote absolute rather than relative permeability and permittivity.

Returning to the CRIM approach described above, for LWD frequencies, CRIM is sensitive to both permittivity and conductive losses [conductive loss is the same as the complex part of the wavenumber $= \frac{\sigma}{\omega \varepsilon}$]. In addition, there is the impact of interfacial polarization between water and matrix. CRIM is not valid without some modification to account for the impact of polarization. The weighted sum of the wavenumber of CRIM is therefore reformulated as follows:

$$k = k_w \cdot \phi \cdot S_w + k_m \cdot (1 - \phi) + k_{hc} \cdot \phi \cdot (1 - S_w) + k_p \cdot \phi \cdot S_{wp} \quad (29)$$

where the index w is water, m is matrix, hc is hydrocarbon, p is interfacial polarization between water and matrix, and wp is interfacial polarized water. The final term of equation (28), $k_p \cdot \phi \cdot S_{wp}$, takes interfacial polarization into account (S_{wp} is the amount

of water that coats the matrix and contributes to the extra polarizations). $\phi \cdot S_{wp} = M_s$ in equation 15.

By applying the electrical properties to the individual elements of Equation (28) it can be shown that (when Φ may be assumed to be small), equation (29) can be reduced to:

$$k \approx k_w \cdot \phi \cdot S_w + k_p \cdot \phi \cdot S_{wp} \quad (30)$$

Equation (30) can be split into real and imaginary parts:

$$k_r = k_{wr} \cdot \phi \cdot S_w + k_{pr} \cdot \phi \cdot S_{wp} \quad (31)$$

$$k_i = k_{wi} \cdot \phi \cdot S_w + k_{pi} \cdot \phi \cdot S_{wp} \quad (32)$$

The polarized water is bounded to the surface of the formation and there are no free charges. Therefore $\sigma_p \approx 0$ and the calculated k_{pr} and k_i by use of Equations (28) are:

$$k_{pr} = \omega \cdot \sqrt{\mu_p \cdot \varepsilon_p} \quad (33)$$

$$k_{pi} = 0 \quad (34)$$

At low frequency, the conductive losses, $\frac{\sigma}{\omega \varepsilon}$, will be far larger than 1 (see Equations(28)). In this case $k_{wr} \approx k_{wi} = k_w$ (see Equation (28)). If k_w and k_{pr} are known, Equations (31) and (32) represent two equations with the two unknowns, S_w and S_{wp} , where S_{wp} is the amount of water that coats the matrix and contributes to an interfacial polarization. Solving Equations (31) and (32) with respect to S_w and S_{wp} gives the following:

$$S_w = \frac{k_i}{k_{wi} \cdot \phi} = \frac{k_i = \omega \sqrt{\mu \varepsilon_{LWD}} \left[\frac{1}{2} \left(\sqrt{1 + \left(\frac{1}{\omega \cdot R_p \varepsilon_{LWD}} \right)^2} - 1 \right) \right]^{1/2}}{k_{wi} \cdot \phi} \quad (35)$$

where k_{wi} is a constant and can be found by tuning S_w (Equation (35)) to be equal to one in shale zones, $k_{wi} = k_i / \phi$, or can be calculated by Equation (28) if R_w and ε_w are known,

and

$$S_{wp} = \frac{k_r - k_i}{k_{pr} \cdot \phi} = \frac{\omega \sqrt{\mu \varepsilon_{LWD}}}{k_{pr} \cdot \phi \cdot \sqrt{2}} \cdot \left[\left[\left(\sqrt{1 + \left(\frac{1}{\omega \cdot R_p \varepsilon_{LWD}} \right)^2} + 1 \right) \right]^{1/2} - \left[\left(\sqrt{1 + \left(\frac{1}{\omega \cdot R_p \varepsilon_{LWD}} \right)^2} - 1 \right) \right]^{1/2} \right]$$

(36)

where k_{pr} can be tuned in zones for where S_w is expected equal S_{wp} .

Considering further Equation (35), ε_{LWD} and R_a are data provided by the service vendor, whilst μ is assumed to be 1, and $\omega = 2\pi f$. The porosity, ϕ , is calculated using the measured density (which can be acquired by either LWD or WL).

5

Figure 6 illustrates the physical zones where this new approach works correctly (radiative part of the near field):

$$\lambda/4\pi < TRS < \lambda, \quad \lambda = \frac{2\pi}{k_r}$$

where TRS is the Transmitter to Receiver Spacing and z is again the coordinate space.

10

Figure 7 illustrates a method of estimating the water saturation level S_w of a region of a subsurface formation surrounding a drilled borehole and comprises the following steps:

S1. Perform an LWD or WL operation to collect phase and amplitude measurements for region surrounding a borehole.

15

S2. Apply an inversion process using an assumed permittivity ε_{LWD} to obtain resistivity data R_a .

S3. Apply a plane wave approximation to the propagation of the electromagnetic signal across the region to extract real k_r and imaginary k_i parts of a wave number k from the resistivity data and the permittivity estimate.

20

S4. Use the extracted real and imaginary parts of the wave number to calculate the water saturation S_w .

It will be appreciated by the person of skill in the art that various modifications may be made to the above described embodiments without departing from the scope of the present invention.

25

CLAIMS:

1. A method of estimating the water saturation level S_w of a region of a subsurface formation surrounding a drilled borehole, the method comprising:

5 obtaining resistivity data determined by analysing the attenuation α of an electromagnetic signal traversing said region and taking into account an assumed electrical permittivity value ε_{LWD} ;

10 applying a plane wave approximation to the propagation of said electromagnetic signal across said region to extract an imaginary part k_i of a wave number k from the resistivity data and said assumed electrical permittivity ε_{LWD} ; and

using the extracted imaginary part of the wave number to calculate water saturation S_w .

15 2. A method according to claim 1, wherein said resistivity data is data obtained by Logging While Drilling or by Wireline and using one or more electromagnetic transmitter and receiver pairs, wherein the transmitter to receiver spacing, TRS, satisfies the condition:

$$\lambda/4\pi < TRS < \lambda,$$

where λ is the wavelength of the transmitted electromagnetic signal.

20

3. A method according to claim 1 or 2, wherein said step of using the extracted imaginary part of the wave number to calculate water saturation comprises calculating water saturation according to the following equation:

$$S_w = \frac{k_i}{k_{wi} \cdot \phi} = \frac{\omega \sqrt{\mu \varepsilon_{LWD}} \left[\frac{1}{2} \left(\sqrt{1 + \left(\frac{1}{\omega \cdot R_a \varepsilon_{LWD}} \right)^2} - 1 \right) \right]^{1/2}}{k_{wi} \cdot \phi}$$

25

, where S_w is the water saturation, k_i is the imaginary part of the wavenumber, k_{wi} is a constant, ϕ is porosity, ω is the angular frequency of the transmitted electromagnetic signal, μ is the electrical permeability, ε_{LWD} is the assumed permittivity value, R_a is a resistivity value of the resistivity data.

30

4. A method according to any one of the preceding claims, and further comprising: obtaining further resistivity data determined by analysing the phase delay δ of the

electromagnetic signal traversing said region and taking into account the assumed electrical permittivity value ε_{LWD} ; and

calculating an amount of water that coats a matrix of said region and contributes to an interfacial polarization according to the following equation:

$$5 \quad S_{wp} = \frac{\omega \sqrt{\mu \varepsilon_{LWD}}}{k_{pr} \cdot \phi \cdot \sqrt{2}} \cdot \left[\left[\left(\sqrt{1 + \left(\frac{1}{\omega \cdot R_p \varepsilon_{LWD}} \right)^2} + 1 \right) \right]^{1/2} - \left[\left(\sqrt{1 + \left(\frac{1}{\omega \cdot R_a \varepsilon_{LWD}} \right)^2} - 1 \right) \right]^{1/2} \right]$$

, where S_{wp} is the amount of water that coats a matrix of said region and contributes to an interfacial polarization, ω is the angular frequency of the transmitted electromagnetic signal, μ is the electrical permeability, ε_{LWD} is the assumed permittivity value, k_{pr} is the real part of a wavenumber associated with the interfacial polarization, ϕ is porosity, R_p is a resistivity value of the further resistivity data, and R_a is a resistivity value of the resistivity data.

5. A method according to any one of the preceding claims and comprising performing a Logging While Drilling operation or a Wireline operation to obtain said resistivity data.

6. A method of drilling a borehole and comprising carrying out Logging While Drilling to obtain resistivity data using the method of any one of the preceding claims to estimate the water saturation level S_w of a region being drilled, and geo-steering a drill bit using the estimated water saturation level to achieve optimal placement of the borehole.

7. A method of estimating the hydrocarbon saturation level S_{HC} of a region of a subsurface formation surrounding a drilled borehole, the method comprising estimating the water saturation level S_w of said region using the method of any one of the preceding claims and using that estimate to estimate said hydrocarbon saturation level.

8. A method of managing a hydrocarbon producing reservoir and comprising determining a water saturation level using the method of any one of claims 1 to 6 or determining a hydrocarbon saturation level according to claim 7, and using the determined water or hydrocarbon saturation level to determine the location and/or orientation of wells into the reservoir, or to determine extraction or injection strategies for the reservoir.

9. A method of determining the electrical permittivity ε_k^f of a region of a subsurface formation surrounding a drilled borehole, the method comprising:

obtaining an assumed electrical permittivity ε_{LWD} ;

5 obtaining resistivity data comprising a first resistivity value R_p determined by analysing the phase delay δ of an electromagnetic signal traversing said region and a second resistivity value R_a determined by analysing the attenuation α of the electromagnetic signal traversing said region; and

10 calculating the electrical permittivity of the region from the first and second resistivity values and the assumed electrical permittivity by applying a plane wave approximation to the propagation of said electromagnetic signal across said region.

10. A method according to claim 9, wherein said resistivity data is obtained by Logging While Drilling (LWD) using one or more electromagnetic transmitter and receiver pairs, wherein the transmitter to receiver spacing (TRS) is within the radiative zone of the near field region of the or each transmitter.

11. A method according to claim 9 or 10, wherein said resistivity data is obtained by Logging While Drilling (LWD) using one or more electromagnetic transmitter and receiver pairs, wherein the transmitter to receiver spacing (TRS) satisfies the condition:

20
$$\lambda/4\pi < \text{TRS} < \lambda,$$

where λ is the wavelength of the transmitted electromagnetic signal, and wherein an antenna of the or each transmitter is equal to or shorter than half the wavelength.

12. A method according to claim 9, 10 or 11, wherein said step of calculating the electrical permittivity comprises calculating the electrical permittivity according to the following equation:

$$\varepsilon = \frac{1}{2} \cdot \varepsilon_{LWD} \cdot [2 + A_p - A_a]$$

, where ε is the calculated electrical permittivity, ε_{LWD} is the assumed electrical permittivity, A_p is a term determined by the first resistivity value, and A_a is a term determined by the second resistivity value.

30

13. A method according to claim 12, wherein

$$A_p = \sqrt{1 + \left(\frac{1}{\omega \cdot R_p \cdot \epsilon_0 \cdot \epsilon_{LWD}}\right)^2}$$

$$A_a = \sqrt{1 + \left(\frac{1}{\omega \cdot R_a \cdot \epsilon_0 \cdot \epsilon_{LWD}}\right)^2}$$

, where ω is the angular frequency of the electromagnetic signal, R_p is the first resistivity value, R_a is the second resistivity value, and ϵ_0 is the electrical permittivity of free space.

14. A method according to claim 9, 10 or 11, wherein the step of calculating the electrical permittivity comprises:

extracting a real part k_r and an imaginary part k_i of a wavenumber from the resistivity data;

using the real and imaginary parts to calculate the electrical permittivity.

15. A method according to claim 14, wherein said step of using the real and imaginary parts comprises calculating the electrical permittivity according to the following equation:

$$\epsilon = \left(\frac{c}{\omega}\right)^2 \cdot \frac{k_r^2 - k_i^2}{\mu}$$

, where ϵ is the calculated electrical permittivity, c is the speed of light in vacuum, ω is the angular frequency of the electromagnetic signal, k_r is the real part of the wavenumber, k_i is the imaginary part of the wavenumber, and μ is the relative permeability of the formation in said region.

16. A method according to any one of claims 9 to 5 and comprising using the calculated electrical permittivity to calculate new resistivity values from the phase delay and the attenuation of the electromagnetic signal.

17. A method according to any one of claims 9 to 16, wherein the resistivity data comprises further resistivity values determined from the phase delay and attenuation of another electromagnetic signal that traversed said region and having a different frequency, and wherein the method further comprises calculating another electrical permittivity of the region from the further resistivity values.

18. A method according to any one of claims 9 to 17 and comprising using the

calculated electrical permittivity to determine a water saturation S_w of the region of the formation.

5 18. A method according to any one of claims 9 to 17 and comprising drilling the borehole, wherein said step of calculating the electrical permittivity is performed while drilling.

10 19. A method according to any one of claims 9 to 18 and comprising geo-steering a drill bit using the determined electrical permittivity to achieve an optimal placement of the borehole.

15 20. A computer device comprising:
a receiver for receiving electromagnetic data; and
a processor arranged to carry out the method of any one of the preceding claims.

20 21. A computer program comprising non-transitory computer readable code which, when run on a computer device, causes the computer device to behave as a computer device according to claim 20.

22. A computer program product comprising a non-transitory computer readable medium and a computer program according to claim 21, wherein the computer program is stored on the non-transitory computer readable medium.

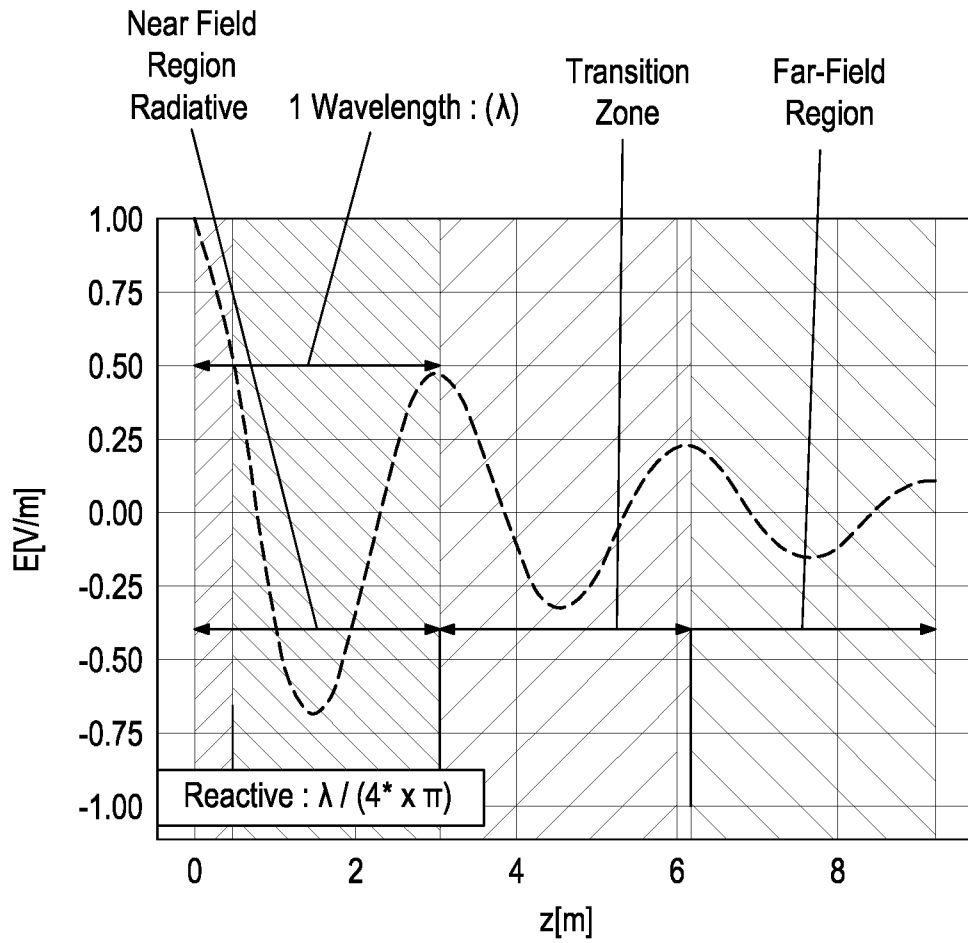


Figure 1

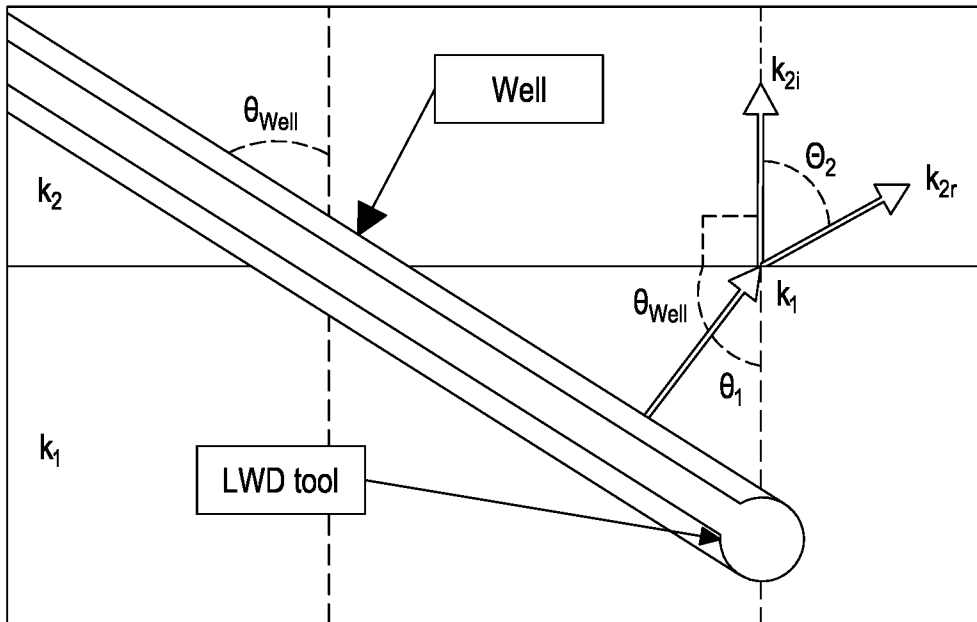


Figure 2

3/6

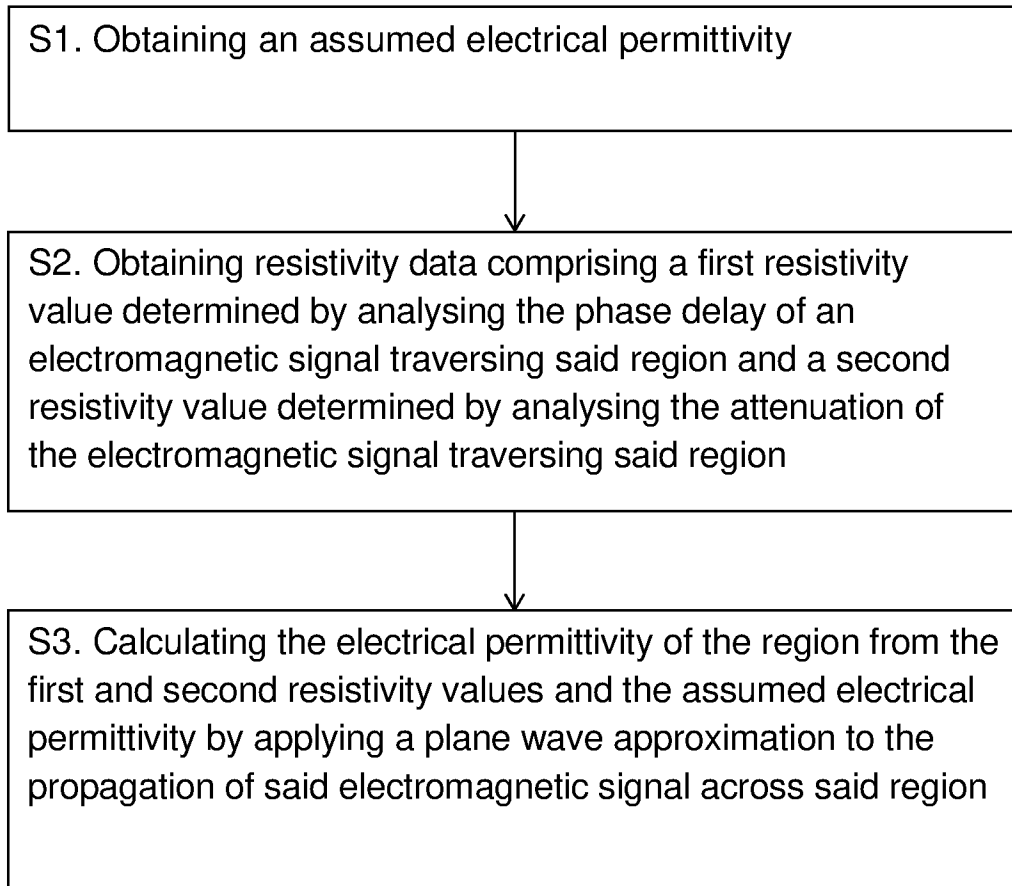


Figure 3

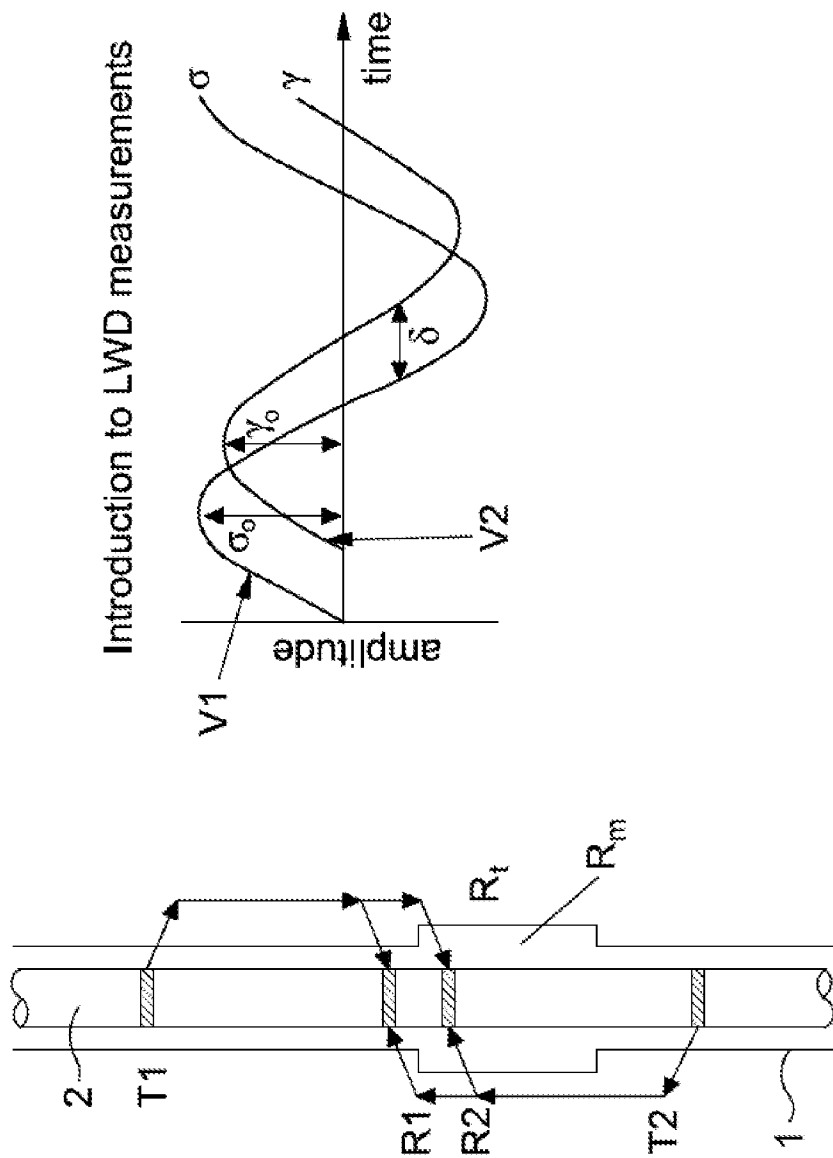


Figure 4

5/6

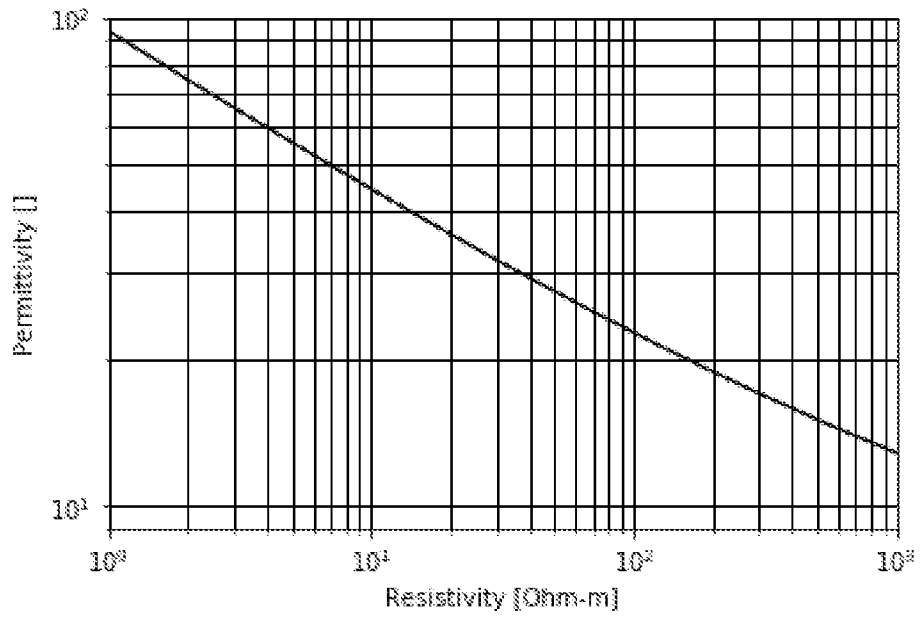


Figure 5

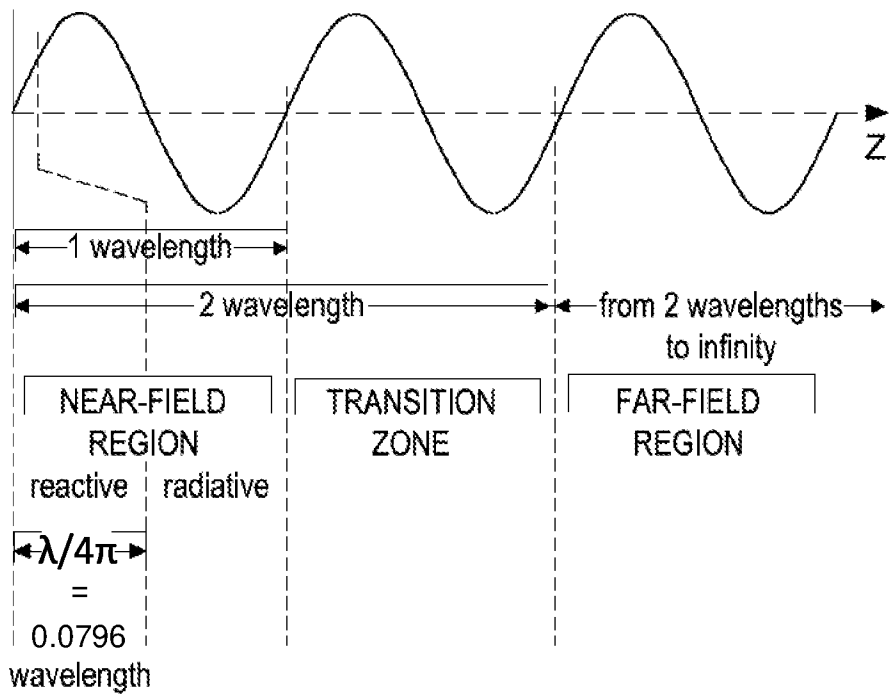


Figure 6

6/6

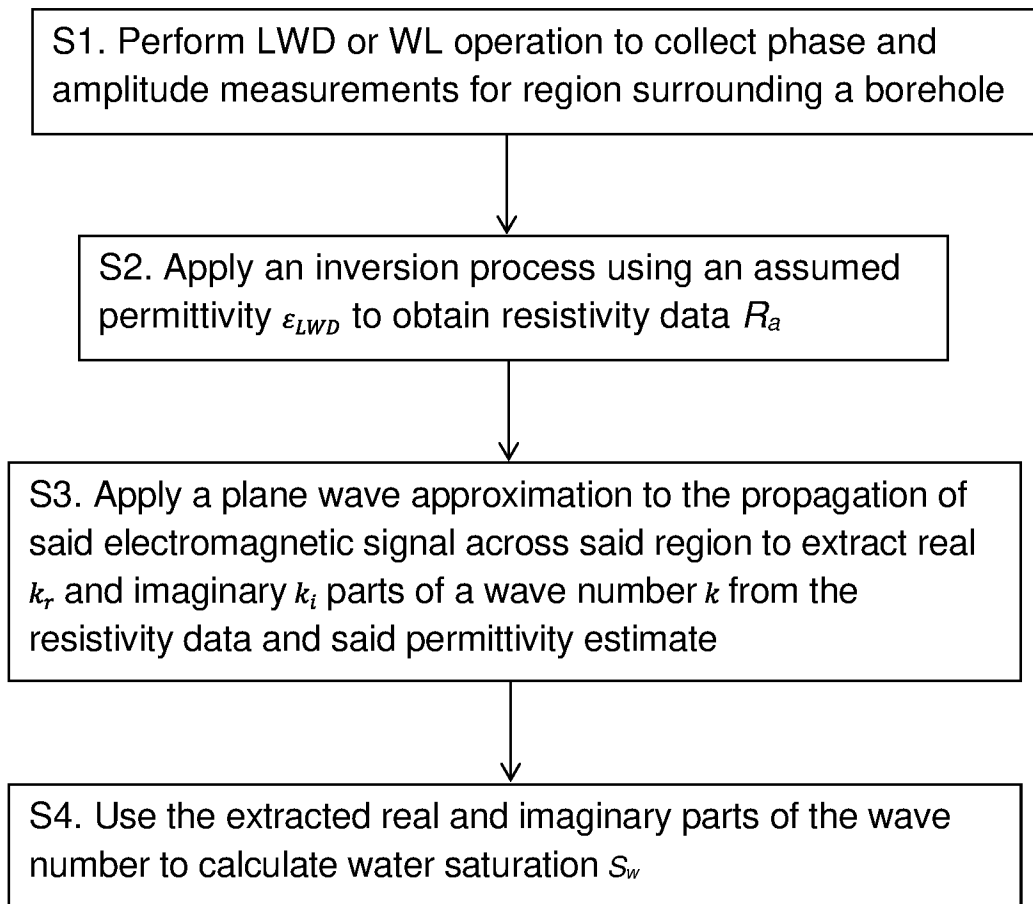


Figure 7

INTERNATIONAL SEARCH REPORT

International application No.

PCT/NO2020/050053

A. CLASSIFICATION OF SUBJECT MATTER		
G01V 3/30 (2006.01), E21B 47/00 (2012.01), G01V 3/38 (2006.01), G01V 3/18 (2006.01)		
According to International Patent Classification (IPC) or to both national classification and IPC		
B. FIELDS SEARCHED		
Minimum documentation searched (classification system followed by classification symbols) G01V, E21B		
Documentation searched other than minimum documentation to the extent that such documents are included in the fields searched DK, NO, SE, FI: Classes as above.		
Electronic data base consulted during the international search (name of data base and, where practicable, search terms used) EPODOC, WPI, FULL TEXT: ENGLISH, GERMAN, FRENCH		
C. DOCUMENTS CONSIDERED TO BE RELEVANT		
Category*	Citation of document, with indication, where appropriate, of the relevant passages	Relevant to claim No.
X	WO 2014/014372 A1 (BAKER HUGHES INC [US]) 2014.01.23	1,5,7,9,14,16-19,21-23
Y	page 5, lines 10-18, page 4, lines 1-5, 15-20, page 10, line 5-page 11, line 21; figure 6-8	2-4,6,8,10-13,15,20
Y	WO 2018/132705 A1 (BAKER HUGHES A GE CO LLC) 2018.07.19 Abstract; appendix; paragraph [00117]-[00118],[0060],[00100]; figure 4b,4c,5b,6a,6b	2-4,6,8,10-13,15,20
Y	WO 2017/165480 A2 (BAKER HUGHES INC [US]) 2017.09.28 Abstract; appendix A; paragraph [0042],[0051]-[0054],[0065]-[0082],[00110]	2-4,6,8,10-13,15,20
A	US 5811973 A (MEYER WALLACE HAROLD JR [US]) 1998.09.22 Entire document, claim set	1-23
P.A	WO 2019/066672 A1 (BAKER HUGHES A GE CO LLC [US]) 2019.04.04 Page 10, line 5 -page12 line 5; claim set	1-23
<input type="checkbox"/> Further documents are listed in the continuation of Box C. <input checked="" type="checkbox"/> See patent family annex.		
* Special categories of cited documents:	"I" later document published after the international filing date or priority date and not in conflict with the application but cited to understand the principle or theory underlying the invention	
"A" document defining the general state of the art which is not considered to be of particular relevance	"X" document of particular relevance; the claimed invention cannot be considered novel or cannot be considered to involve an inventive step when the document is taken alone	
"D" document cited by the applicant in the international application	"Y" document of particular relevance; the claimed invention cannot be considered to involve an inventive step when the document is combined with one or more other such documents, such combination being obvious to a person skilled in the art	
"E" earlier application or patent but published on or after the international filing date	"&" document member of the same patent family	
"L" document which may throw doubts on priority claim(s) or which is cited to establish the publication date of another citation or other special reason (as specified)		
"O" document referring to an oral disclosure, use, exhibition or other means		
"P" document published prior to the international filing date but later than the priority date claimed		
Date of the actual completion of the international search	Date of mailing of the international search report	
30/03/2020	17/04/2020	
Name and mailing address of the ISA Nordic Patent Institute Helgeshøj Allé 81 DK - 2630 Taastrup, Denmark. Facsimile No. -	Authorized officer Bill Arlander Telephone No. +47 22387 524	

INTERNATIONAL SEARCH REPORT
Information on patent family members

International application No.

PCT/NO2020/050053

Patent document cited in search report / Publication date	Patent family member(s) / Publication date
WO 2014014372 A1 2014.01.23	US 2014019049 A1 2014.01.16 US 9581720 B2 2017.02.28 NO 20150037 A1 2015.01.07 GB 2519268 AB 2015.04.15 BR 112014030358 A2 2017.06.27
WO 2018132705 A1 2018.07.19	US 2018203151 A1 2018.07.19 NO 20190896 A1 2019.07.17 GB 2573918 A 2019.11.20 BR 112019014132 A2 2020.02.11
WO 2017165480 A2 2017.09.28	WO 2017165480 A3 2017.09.28 US 2017276832 A1 2017.09.28 NO 20181295 A1 2018.10.09 GB 2564795 A 2019.01.23 BR 112018068583 A2 2019.02.12
US 5811973 A 1998.09.22	US 5869968 A 1999.02.09 GB 2301442 AA8B 1996.12.04 GB 2322201 AB 1998.08.19 GB 2322200 AB 1998.08.19 GB 2322199 AB 1998.08.19 GB 2322198 AB 1998.08.19
WO 2019066672 A1 2019.04.04	US 2019094405 A1 2019.03.28